Removal of Acid Red dye from aqueous solution using zero-valent copper and zero-valent zinc nanoparticles

Mohamed Abdel Salam*, Samia A. Kosa, Nouf A. Al-Nahdi, Nuha Y. Owija

Chemistry Department, Faculty of Science, King Abdulaziz University, P.O Box 80200-Jeddah 21589, Saudi Arabia,
Tel. +966-541886660, Fax +966-2-6952292, email: masalam16@hotmail.com (M.A. Salam), Tel. +966-557627075, Fax +966-2-6952292,
email: skousah@kau.edu.sa (S.A. Kosa), Tel. +966-550434874, Fax +966-2-6952292, email: chamical88@hotmail.com (N.A. Al-Nahdi),
Tel. +966-501694384, Fax +966-2-6952292, email: nuhaawija@hotmail.com (N.Y. Owija)

ABSTRACT

In this research, different zero-valent metal nanoparticles were synthesized, zinc nanoparticles (ZnNPs), copper nanoparticles (CuNPs) via reduction route using sodium borohydide, and used for the removal of Acid Red dye (AR dye); as an example or organic dyes, from aqueous solution. The prepared NPs were characterized, and the results confirmed the presence of the nanoparticles, and their chemical composition was identified. The effect of different experimental conditions was explored, and the results showed that most of the AR dye could be removed from solution within few minutes, at ambient temperature using most 80 mg ZnNPs, 30 mg of CuNPs. The removal of the AR dye using ZnNPs, and CuNPs, was studied kinetically and thermodynamically, and the results showed that the experimental data were best fitted using the pseudo-second-order kinetic model with excellent correlation coefficients. The thermodynamic study of the removal process showed the spontaneity of the process. The mechanism of the removal process was studied, and the results showed that the removal process occurred via reductive catalytic degradation of the AR dye molecules by the NPs. Finally, the prepared ZnNPs and CuNPs were used for the removal of AR dye in real wastewater sample, and the results showed the high removal efficiency.

Keywords: Acid Red dye; Copper nanoparticles; Removal; Wastewater; Zinc nanoparticles

1. Introduction

Many industries depend greatly on organic dyes, and currently, there is more than one hundred thousand type of the dyes are extensively used, with massive annual production exceeds 0.7 million tons, and a considerable amount of these dyes being released to the aquatic environment during the industrial process [1]. Moreover, conventional wastewater treatment protocols cannot remove these persistent dyes which characterized with high stability to the different environment such as light, temperature, water, and detergents [2]. Accordingly, the released dyes had their adverse effect on the environment due to their toxicity, carcinogenicity, and mutagenicity [3,4]. Also, due

to their intense colors, water pollution with dyes reduces sunlight penetration, which reduces the aquatic plant photosynthesis which reduces the growth of the plants and the substantial death of plants, which accordingly can cause a fish death due to oxygen depletion. For these reasons, it is crucial to treat industrial effluents, and wastewater contains dyes to avoid such health and environmental complications. Conventional chemical dye removal methods are advanced oxidation process, electrochemical destruction, Fenton reaction dye removal, oxidation, ozonation, photochemical and ultraviolet irradiation [5–8]. In recent years, zero-valent metal usually used for the catalytic degradation of organic pollutants in water reduction process which is a redox process were the metal acts as an electron donor for the reduction of organic pollutants. Although, most of the research work used zero-valent iron for the reductive catalytic degradation of different organic com-

*Corresponding author.

pounds in water such as dyes [9–17], and natural organic matter [18], but there few studies focus on the reductive catalytic degradation using other zero-valent metals. For example, zero-valent zinc was used for the reductive catalytic degradation of chlorinated phenols [19], 1,2,3-trichloropropane [20], and n-nitrosodimethylamine [21] in water, where as zero-valent silver was used for the catalytic degradation of organic dyes [22,23]. Also, zero-valent copper was used as an efficient catalyst for the reductive catalytic degradation of methylene blue dye [24,25], methyl orange [26–28], Congo red [28].

In this research paper, different zero-valent metal nanoparticles were synthesized; zinc nanoparticles (ZnNPs), and copper nanoparticles (CuNPs).The prepared NPs were characterized using different characterization techniques; SEM-EDS, TEM, XRD, and surface area analysis, to explore their morphology, chemical, and physical properties. The prepared NPs were used for the removal of Acid Red 1 Dye (AR dye); as an example of organic azo dyes, from aqueous solution. Acid Red 1 dye; also called Red 2G,is a synthetic monoazo dye which was banned by the European Union due to its high toxicity and carcinogenic effects [29]. The effect of different environmental conditions, NPs mass, removal time, and solution temperature were investigated. Additionally, the removal process was studied kinetically and thermodynamically to predict the removal rate to understand the removal behavior, the mechanism of removal, and its spontaneity by calculating different thermodynamic parameters. The mechanism of the removal process was discussed according to the degradation of the AR dye and the total organic carbon (TOC) measurements.
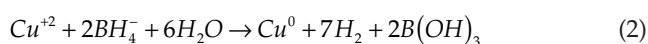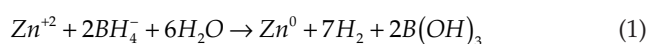
2. Experimental section

2.1. Materials

All chemical were obtained from SIGMA-ALDRICH, were general purpose reagents; sodium borohydride, zinc chloride, and copper (II) sulphate, used for the preparation of CuNPs, and ZnNPs. All solutions were prepared by deionized water.

2.2. Synthesis of ZnNPs and CuNPs

The zero-valent copper nanoparticles were prepared by adding $CuSO_4 \cdot H_2O$ (0.04 M) solution drop wise into the $NaBH_4$ (0.13 M) solution, resulting in the formation of a black precipitate of CuNPs. The zero-valent zinc nanoparticles were prepared by adding $ZnCl_2$ (0.04 M) solution drop wise into the $NaBH_4$ (0.13 M) solution, resulting in the formation of white precipitate of ZnNPs. The precipitated NPs then was harvested by vacuum filtration and washed with 1000 ml deionized water, then dried overnight at 110°C. All solutions were prepared with deionized water, and the reaction solution was fully mixed by a magnetic stirrer at room temperature. The reaction of ZnNPs and CuNPs preparation could be as the following:

$$Zn^{+2} + 2BH_4^- + 6H_2O \rightarrow Zn^0 + 7H_2 + 2B(OH)_3 \qquad (1)$$

$$Cu^{+2} + 2BH_4^- + 6H_2O \rightarrow Cu^0 + 7H_2 + 2B(OH)_3 \qquad (2)$$

2.3. Preparation of AR dye solution

The stock solution of Acid Red 1 dye (Fig. 1, chemical formula: $C_{18}H_{13}N_3Na_2O_8S_2$; and $\lambda_{max} = 553$); was prepared by dissolving 0.0200 mg of the dye in 1 L of deionized water.

2.4. Characterization techniques

The sample morphology and micro-analysis were performed using SEM equipment Hitachi instrument, Model TM-1000 equipped by an energy disperse X-ray spectrometer (EDS). A transmission electron microscope (TEM; type JEOL JEM-1230, operating at120 kV, attached to a CCD camera). Philips X-pert Pro diffractometer was used for X-ray diffraction (XRD) patterns operated at 40 mA and 40 kV by using CuKα radiation in the 2θ range from 2 to 80°. The specific surface areas of the NPs were determined from nitrogen adsorption/desorption isotherms which were measured at 77 K by using a Nova 2000 series Chromatech. Before analysis, the samples were out gassed at 300°C for 4 h.

2.5. Removal study

Adsorption experiments were performed to determine the effect of different parameters affecting the adsorption of acid red dye by the NPs under different environmental conditions. The experimental procedures were performed as follows: (1) a series of solutions of AR dye was prepared; (2) the initial pH was measured, and a defined amount of the NPs was then added to the solutions; (3) these solutions were agitated on a magnetic stirrer for a certain period of time, at room temperature; (4) at defined points in time, a certain volume of the solution was removed and immediately filtered to collect the supernatant; and (5) the residual AR dye concentration in the supernatant using UV/Vis spectrophotometer at 553 nm. The amount of AR dye removed by ZVNPs was determined from the difference of the initial concentration ($C°$) and the equilibrium concentration (C_t). The percentage removed of AR dye from the solution was calculated using the following equation:

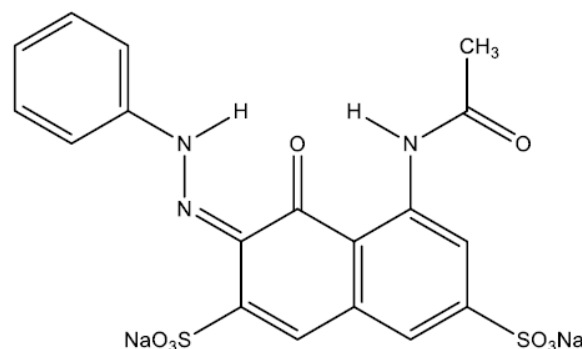$$\% \, Removed = \frac{(C_\circ - C_t)}{c_\circ} \times 100 \qquad (3)$$

Fig. 1. Chemical structure of Acid Red 1 dye.

The amount AR dye removed from solution per unit mass of the NPs (q_t; mg/g),) was calculated using the following equation:

$$q_t = \frac{(C_\circ - C_t)}{m}V \qquad (4)$$

where $C_\circ$ is the initial AR dye concentration (mg/L), C_t is the AR dye concentration at certain time (mg/L), V is the volume of solution (L), and m is the mass of NPs (g).

It is noteworthy to mention that all the experiments were repeated three times, and the reported values were the average with less than 5% error.

3. Results and discussion

3.1. Characterization of ZnNPs, and CuNPs

The structure and composition of the prepared ZnNPs and CuNPs were investigated using SEM/EDS, TEM, XRD, and surface area analysis. Fig. 2 shows the morphological structures of the prepared ZnNPs and CuNPs using SEM
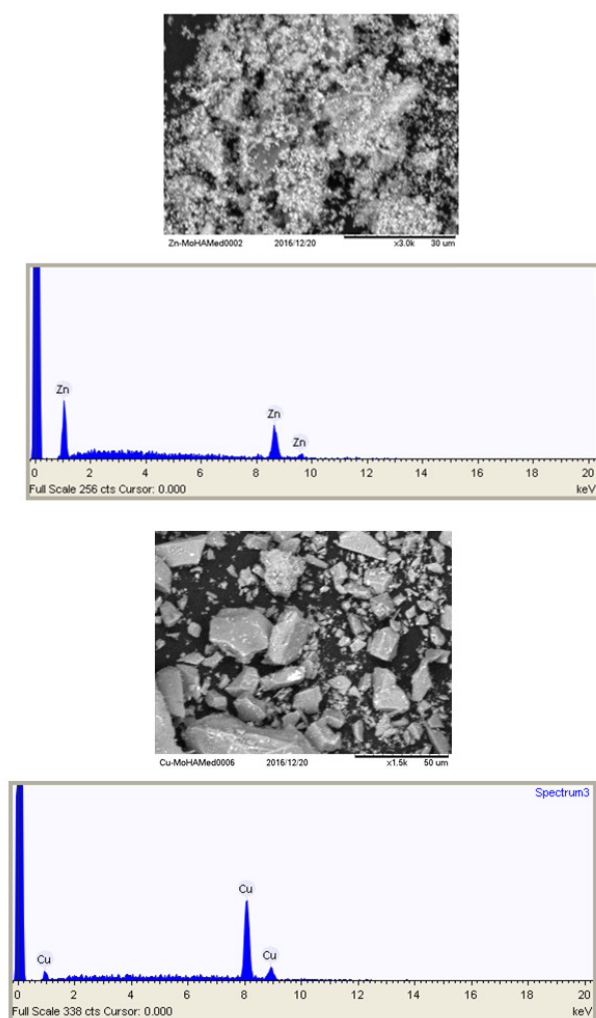

Fig. 2. SEM image, and EDS spectrum of the ZnNPs, and CuNPs.

equipped with EDS. The figure showed that ZnNPs exist as an agglomeration of spherical nanoparticles, and due to the microscope power limitations, the particle size could not be estimated. The EDS spectrum showed that the nanoparticles were composed of 100% zinc; zero-valent ZnNPs. Also, the figure showed that CuNPs exist as an agglomeration of plates, and again due to the microscope power limitations, the particle size could not be estimated. The EDS spectrum showed that the nanoparticles were composed of 100% copper; zero-valent CuNPs. Fig. 3 shows the TEM images at different magnifications of the ZnNPs, which were spherical in shape with non-uniform size, tend to agglomerate, with an average diameter of 200 nm. Also, using higher magnification power showed that a single spherical nanoparticle could be a collection of smaller particles. The TEM showed that CuNPs were elongated double-cone in shape with non-uniform size, with an average diameter of 50 nm at the middle, and few hundred nanometers in length as it is clear from Fig. 4. The XRD pattern of the ZnNPs and CuNPsis shown in Fig. 5. The XRD pattern of the ZnNPs was consistent with that of Wurtzite structure of zincite (ZnO, ref. JCPDS 01-079-0206) and not zero-valent zinc which could be attributed to the high reactivity of the prepared ZnNPs, and the extended period between the preparation time and the XRD measurements. The average crystallite size was estimated using the Scherrer equation and was 220 nm. Meanwhile, in the case of CuNPs XRD pattern, Cu(0) was identified from three obvious diffraction peaks at $2\theta = 43.3$, 50.3, and $73.8°$, which corresponded to the (111), (200), and (220) crystal planes of face-centered cubic (fcc) copper, respectively (JCPDS No. 01-085-1326).The average crystallite size was estimated using the Scherrer equation, and was30 nm. The specific surface area of the ZnNPs and CuNPs were determined using nitrogen adsorption/desorption isotherms and were found to be 16.1 m²/g, and 71.3 m²/g, respectively, indicating the large specific surface area of the CuNPs compared with the ZnNPs.

3.2. Removal study

The effects of different parameters affected the removal of AR dye by ZnNPs and CuNPs from an aqueous solution were investigated and optimized. The effect of NPs mass on the removal of AR dye from aqueous solution was studied, and the results were presented in Fig. 6. The experimental results revealed that AR dye removal increased gradually with increasing the amount of NPs used, and most of the AR dye was removed from the solution using 80 mg ZnNPs; 95.6%, and30 mg of CuNPs; 95.5%, and further increased in the amount of NPs used associated with 100% removal of AR dye from solution. This may be attributed to the fact that increasing the NPs mass provides a greater surface area or more removal sites for the AR dye. Also, CuNPs are more efficient for the removal AR from solution compared with the ZnNPs. This is may be due to the high surface area of the CuNPs compared with the ZnNPs; 16.1 m²/g, and 71.3 m²/g, respectively. Also, the great stability of the CuNPs compared with the ZnNPs as was confirmed by the XRD measurements, make the CuNPs be more efficient degradation of the AR dye.

The contact time is one key factor affecting the removal of any pollutants from the environment. The effect of the
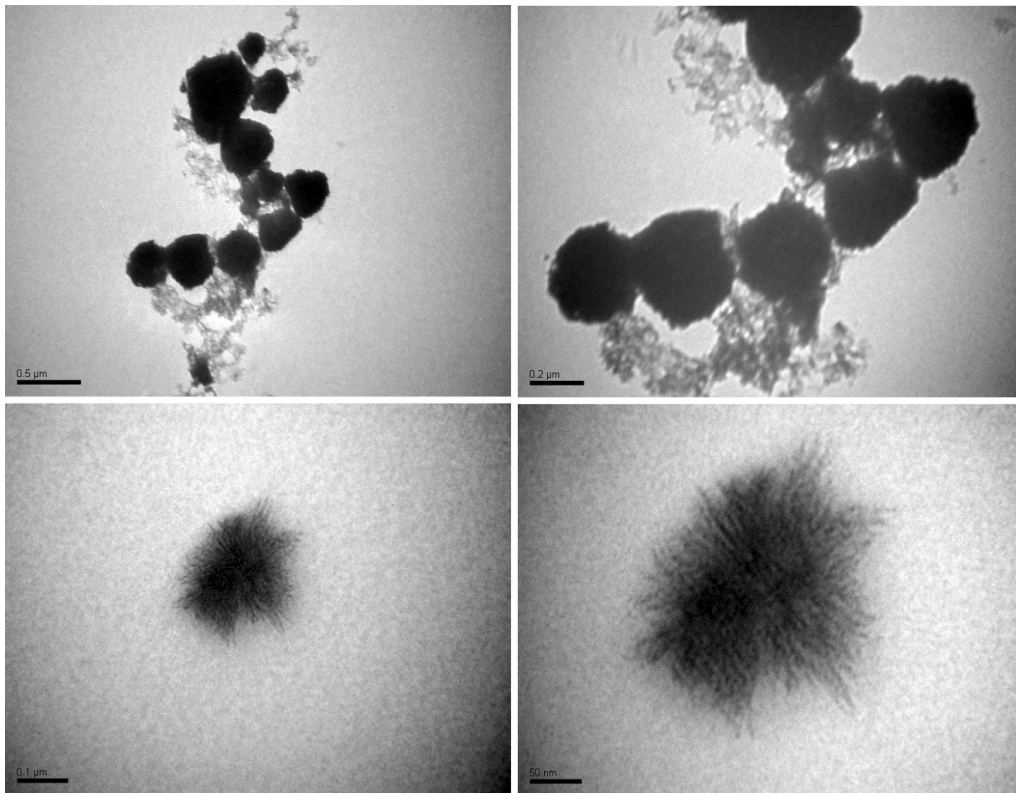
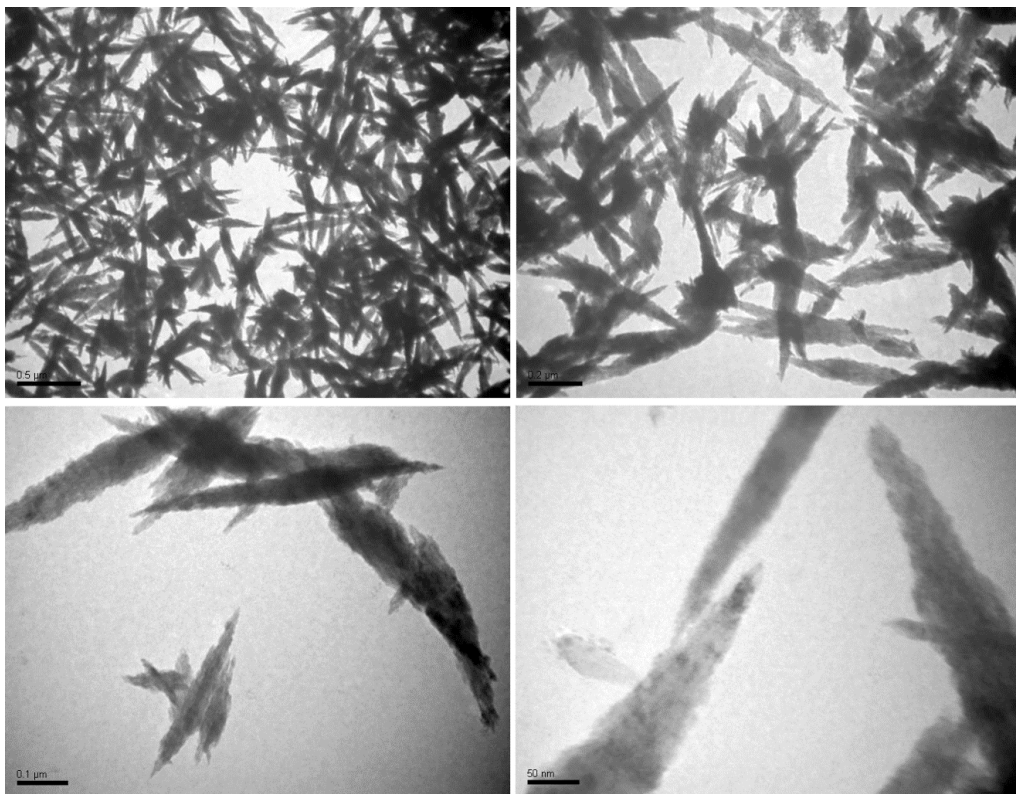Fig. 3. TEM images of the ZnNPs at different magnifications.

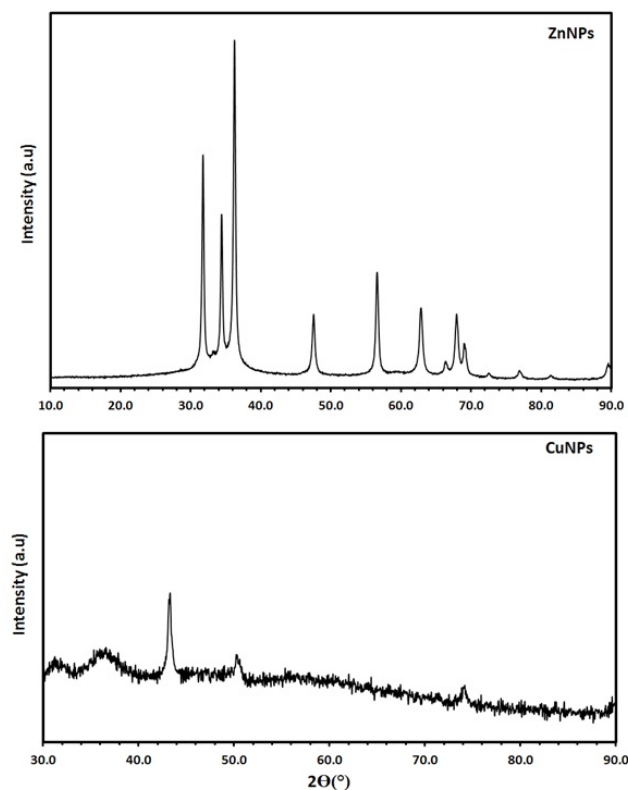Fig. 4. TEM images of the CuNPs at different magnifications.
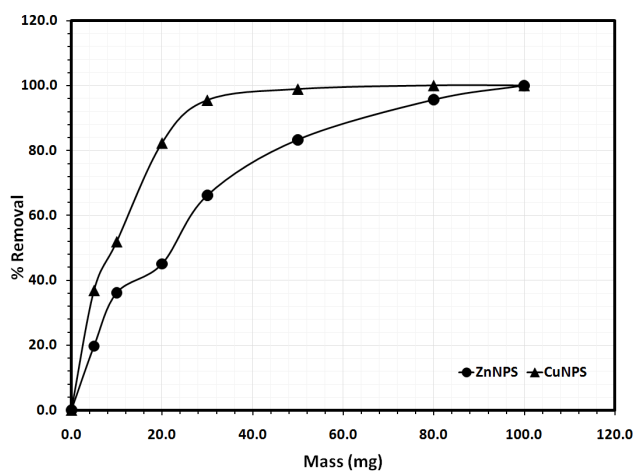
Fig. 5. XRD pattern of the ZnNPs, and CuNPs.

Fig. 6. Effect of ZnNPs, and CuNPs mass on the AR dye removal from an aqueous solution. (Experimental conditions: 20.0 ml solution, pH 8.0, 60 min, 298 K, and AR dye concentration 20.0 mg L^{-1}).
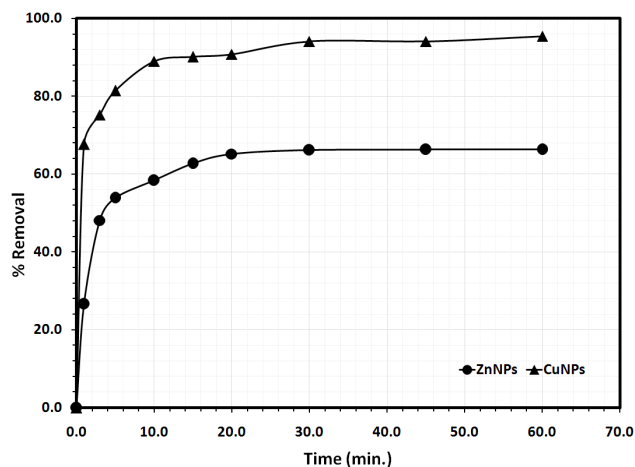

Fig. 7. Effect of contact time on the AR dye removal from an aqueous solution by ZnNPs and CuNPs. (Experimental conditions: 30.0 mg ZnNPs, 20.0 mg CuNPs, 20.0 ml solution, pH 8.0, and AR dye concentration 20.0 mg L^{-1}).

contact time on the AR dye removal from model solution by NPs was studied, and the results are shown in Fig. 7. In the case of ZnNPs, it is was noted that the percentage removal of the AR dye increased remarkably within the first 10 min with 58.4% removal, and then reached equilibrium within 30 min with a maximum removal of 66.2%, and further increase in the contact time did not change significantly

the % AR dye removal, which reached 66.3% after 60 min. In the case of CuNPs, It is was noted that the percentage removal of the AR dye increased remarkably within the first 5 min with 81.5% removal, and reached equilibrium within 10 min with a maximum removal of 90.2%. Further increase in the contact time did not change significantly the % AR dye removal, which reached 95.5% after 60 min. Accordingly, the equilibrium time was assigned as 60 min for the rest of the experiments to assure that equilibrium was achieved.

In order to understand the removal process and either if it is photolysis; degradation of dye due to light or other radiant energy, photo catalytic; degradation of dye due to light or other radiant energy due to the presence of photo catalyst, or catalytic degradation; degradation of dye due to the presence of catalyst in absence or presence of light or other radiant energy. A comparison was performed between AR dye solutions on the visible light inside the laboratory without the NPs (photolysis), with the NPs in visible light (photo catalytic), and finally with the NPs in dark conditions (catalytic degradation). It was observed that AR dye was stable in the presence of visible light within the experimental time window, and the % of AR decomposed due to photolysis was less than 1.0%, indicating that the degradation of the AR dye is not a photolysis process. Also, the % AR removed from solution was almost the same with the NPs in the presence and absence of the light, indicating that the removal of the AR dye from solutions by both NPs is mainly due to catalytic degradation. To differentiate between the catalytic degradation and the adsorption of the AR dye by both NPs, it was clear that the ZnNPs white color did not change upon the removal process, and the solid black CuNPs was added to different solvents; methanol, acetone, ethanol, DMF, hexane, but no AR dye was desorbed. This may indicate that the removal of the AR dye by both ZnNPs and CuNPs was solely due to catalytic degradation process. The same phenomenon was observed when the zero-valent iron was used for the removal of different azo dyes, as the removal due to

adsorption was insignificant compared with the reductive catalytic degradation process [10].

The solution temperature is one of the major factors, which affect the removal process, in many ways, as it decreases the solution density and enhances the diffusion ability of the pollutant, which facilitate the interaction with the solid NPs. The effect of solution temperature on the removal of AR dye by ZnNPs and CuNPs was studied at different temperatures in the range between 278 K and 316 K, and the results are presented in Fig.8. It is clear from the figure that raising the solution temperature significantly affected the percentage of AR dye removed from solution by ZnNPs. Increasing the temperature from 278 K to 316 K accompanied by a gradual increase in the percentage of AR dye removed from the solution by ZnNPs; raising the solution temperature from 278 K to 316 K was associated with an enhancement in the % AR dye removed from 59.4% to 69.1%, respectively. In the case of CuNPs, it is clear from the figure that raising the solution temperature significantly affected the percentage of AR dye removed from solution by CuNPs. Increasing the temperature from 278K to 316K accompanied by a gradual increase in the percentage of AR dye removed from the solution by CuNPs; raising the solution temperature from 278 K to 316 K was associated with an enhancement in the % AR dye removed from 61.5% to 97.0%, respectively. This may indicate the endothermic nature of the removal process, as the % AR dye removed increased by raising the solution temperature. Further discussion will be continued in the thermodynamic study. This may indicate the endothermic nature of the removal process, as the % AR dye removed increased by raising the solution temperature. Further discussion will be continued in the thermodynamic study.

3.3. Kinetic studies

An appropriate mathematical kinetic model is important to describe the interactions of the pollutants with the solid NPs to develop the suitable NPs materials for indus-trial applications. Fig. 9 shows the variation of the amount AR dye removed from aqueous solution by NPs (q_t) with time. It is clear from the figure that the removal of AR dye by both NPs reached equilibrium within 10 min and the amount of AR dye removed per unit mass of NPs was 11.9 mg/g, and 7.78 mg/g, for the CuNPs, and ZnNPs, respectively. These amounts were slightly increased to 12.73 mg/g, and 8.84 mg/g, for the CuNPs, and ZnNPs, respectively, after 60 min. The experimental data were kinetically treated using the normal first order and second order kinetic models which could be suitable for the degradation of AR dye by NPs via a catalytic degradation pathway, but unfor-tunately, none of the models was fitted as the equilibrium was attained within few minutes. Therefore, the removal experimental data were treated kinetically using the most common and well-known kinetic models, Lagergren pseu-do-first-order kinetic model, and pseudo-second-order kinetic model [30].

Lagergren pseudo-first-order kinetic model is one of the most frequent kinetic models used to describe the removal of different pollutants from an aqueous solution by solid NPs, and it's linearized for as the following:

$$\ln(q_e - q_t) = \ln q_e - k_1 T \tag{5}$$

where k_1 (min^{-1}) is the pseudo-first-order removal rate coef-ficient, and q_e and q_t are the values of the amount removed per unit mass at equilibrium and at any time t, respectively. By applying Eq. (5) to the experimental data removal by ZnNPsin Fig. 10, and plotting ln ($q_e - q_t$) vs. t gave a straight line, with high convergence, and acceptable R^2 value, as it is shown in Fig. 10, and Table 1. But, unfortunately, the there was not a good agreement between the calculated and experimental amount AR dye removed per unit mass of ZnNPs at equilibrium, which demonstrated the unsuit-ability of Lagergren pseudo-first-order kinetic model for describing the removal of the AR dye on ZnNPs from aque-ous solution. Also, by applying Eq. (5) to the experimental removal by CuNPs in Fig. 10, and plotting ln ($q_e - q_t$) vs.
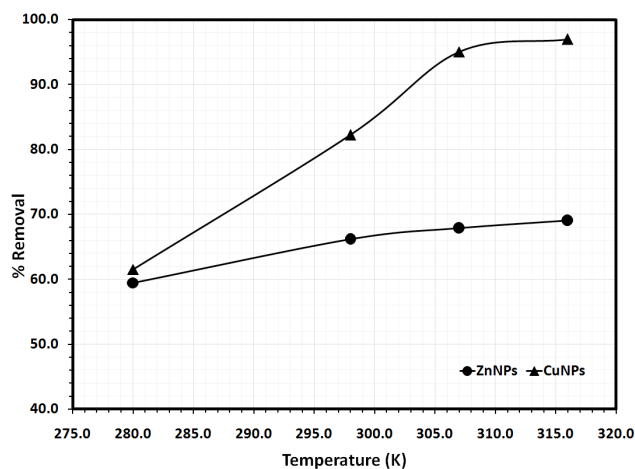

Fig. 8. Effect of solution temperature on the AR dye removal from an aqueous solution by ZnNPs and CuNPs. (Experimental conditions: 30.0 mg ZnNPs, 20.0 mg CuNPs, 20.0 ml solution, 60 min, pH 8.0, and AR dye concentration 20.0 mg L^{-1}).
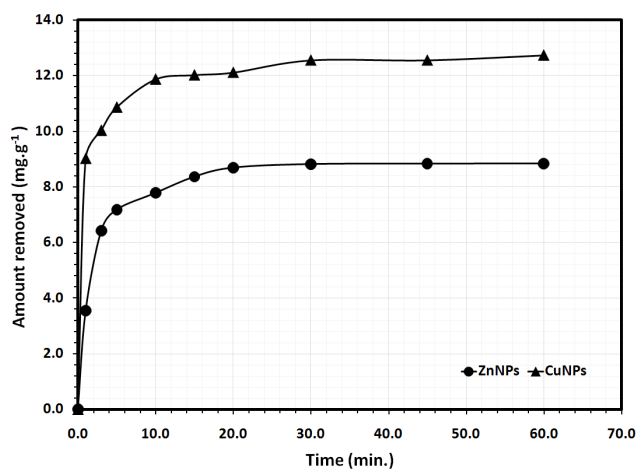

Fig. 9. Variation of the amount AR dye NPs per unit mass of ZnNPs and CuNPs(q_t) with time. (Experimental conditions: 30.0 mg ZnNPs, 20.0 mg CuNPs, 20.0 ml solution, pH 8.0, 298 K, and AR dye concentration 20.0 mg L^{-1}).
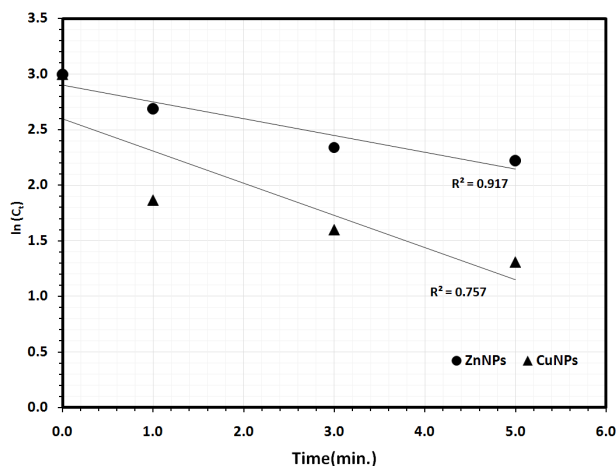
Fig. 10. The application of first-order kinetic model for the AR dye removal from an aqueous solution by ZnNPs and CuNPs. (Experimental conditions: 30.0 mg ZnNPs, 20.0 mg CuNPs, 20.0 ml solution, pH 8.0, 298 K, and AR dye concentration 20.0 mg L^{-1}).
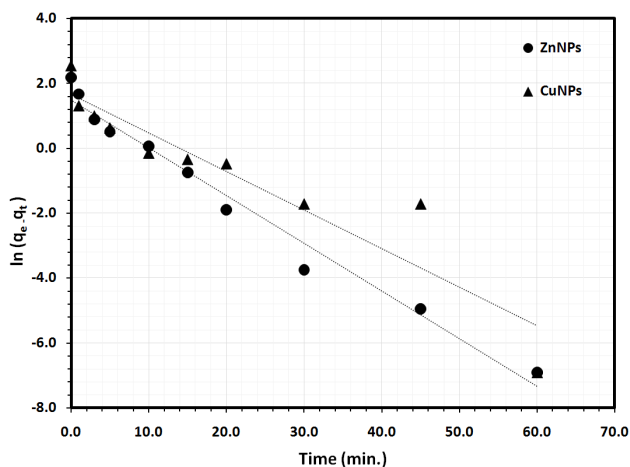

Fig. 11. The application of pseudo-first-order kinetic model for the AR dye removal from an aqueous solution by ZnNPs and CuNPs. (Experimental conditions: 30.0 mg ZnNPs, 20.0 mg CuNPs, 20.0 ml solution, pH 8.0, 298 K, and AR dye concentration 20.0 mg L^{-1}).

Table 1
Different kinetic models parameters for the AR dye NPs from an aqueous solution by ZnNPs and CuNPs

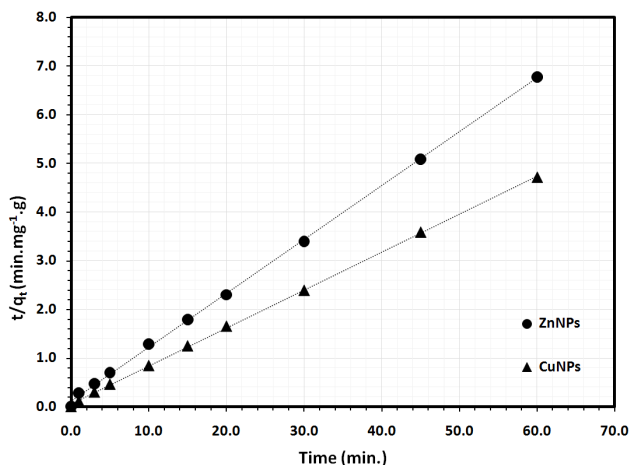| ZnNPs				
Pseudo-first-order kinetic model				
k_1	$q_{e,exp}$ (mg/g)	$q_{e,calc}$ (mg/g)	χ^2	R^2
0.147	8.84	4.42	4.42	0.978
Pseudo-second-order kinetic model				
k_2 (g/mg·min)	$q_{e,exp}$ (mg/g)	$q_{e,calc}$ (mg/g)	χ^2	R^2
0.106	8.84	9.02	0.004	0.999
CuNPs				
Pseudo-first-order kinetic model				
k_1	$q_{e,exp}$ (mg/g)	$q_{e,calc}$ (mg/g)	χ^2	R^2
0.120	12.73	5.29	0.0003	0.873
Pseudo-second-order kinetic model				
k_2 (g/mg·min)	$q_{e,exp}$ (mg/g)	$q_{e,calc}$ (mg/g)	χ^2	R^2
0.115	12.73	12.79	10.5	0.978

Fig. 12. The application of the pseudo-second-order kinetic model for the AR dye removal from an aqueous solution by Zn-NPs, CuNPs. (Experimental conditions: 30.0 mg ZnNPs, 20.0 mg CuNPs, 20.0 ml solution, pH 8.0, 298 K, and AR dye concentration 20.0 mg L^{-1}).

t did not give a straight line, low convergence, and unacceptable R^2 value, as it is shown in Fig. 10, and Table 1. At the same time, the agreement between the calculated and experimental amount AR dye removed per unit mass of CuNPs at equilibrium was very low, which demonstrating the unsuitability of Lagergren pseudo-first-order kinetic model for describing the removal of the AR dye on CuNPs from aqueous solution.

The linearized equation of the pseudo-second-order kinetic model equation is given as:

$$\frac{1}{q_t} = \frac{1}{k_2 q_e^2} + \frac{1}{q_e} \qquad (6)$$

where k_2 (g/(mg·min)) is the pseudo-second-order rate coefficient. Applying the pseudo-second-order kinetic model equation to the removal experimental data by ZnNPs in Fig. 9, by plotting of t/q_t and t of Eq. (6), converged well, with excellent R^2 value, and a straight line was obtained from which q_e and k_2 were estimated from the slope and intercept of the plot, respectively, as it is presented in Fig. 12, and Table 1 confirmed the suitability of the pseudo-second-order kinetic model for the description the removal of AR dye by ZnNPs from aqueous solution. Meanwhile, applying the pseudo-second-order kinetic model equation to the removal experimental data by CuNPs in Fig. 9, by plotting of t/q_t and t of Eq. (6), converged well, with excellent R^2 value, and a straight line was obtained from which q_e and k_2 were estimated from the slope and intercept of the plot, respectively, as it is presented in Fig. 12, and Table 1, con-

firmed the suitability of the pseudo-second-order kinetic model for the description the removal of AR dye by CuNPs from aqueous solution. Another test was performed to confirm the suitability of the pseudo-second-order kinetic is by calculating the Chi-square test using the following mathematical equation [31]:

$$\chi^2 = \sum \frac{(q_{e,calc} - q_{e,exp})^2}{q_{e,calc}} \tag{7}$$

where $q_{e,exp}$ and $q_{e,calc}$ are the calculated and experimental amount of AR dye removed per unit mass of NPs at equilibrium, respectively. Accordingly, in the case of ZnNPs, the χ^2 value for the pseudo-second-order kinetic model was 0.004, whereas it was 4.42 when the pseudo-first-order kinetic model was applied, indicating the appropriateness of the pseudo-second-order kinetic model. Also, in the case of CuNPs, the χ^2 value for the pseudo-second-order kinetic model was 0.0003, whereas it was 10.5 when the pseudo-first-order kinetic model was applied, indicating the appropriateness of the pseudo-second-order kinetic model.

Based on the above results, it could conclude here that pseudo-second-order kinetic model was the best for describing the removal of AR dye from aqueous solution by ZnNPs, and CuNPs compared with the other kinetic models.

A comparison of the different techniques used for the removal of different Acid Red dyes was performed and is presented in Table 2. It is clear from the table that the catalytic degradation of AR dye by ZnNPs, and CuNPs are very competitive to other removal methods based on the removal capacity and the treatment time.

3.4. Thermodynamic studies

Thermodynamic parameters; enthalpy change (ΔH), entropy change (ΔS), and Gibbs free energy change (ΔG), were calculated to evaluate the thermodynamic feasibility and the spontaneous nature of the AR dye molecules by the ZnNPs from aqueous solution. Thermodynamic parameters were calculated using the variation of the thermodynamic distribution coefficient D with a change in temperature according to the equation [32]:

$$D = \frac{q_e}{C_e} \tag{8}$$

where q_e is the amount of AR dye molecules removed by the NPs (mg/g) at equilibrium, and C_e is the equilibrium concentration of AR dye in solution (mg/L). The ΔH and ΔS could be calculated according to the following equation:

$$\ln D = \frac{\Delta S}{R} - \frac{\Delta H}{RT} \tag{9}$$

In the case of ZnNPs, a straight line was obtained by plotting $\ln D$ vs. $1/T$; as it is shown in Fig. 13, and the ΔH and ΔS values were calculated from the slope and the intercept of the straight line, respectively. The ΔG value was calculated at 298K from the relation:

$$\Delta G = \Delta H - T\Delta S \tag{10}$$

Thermodynamic parameters for the removal of AR dye molecules removed by the ZnNPs were calculated, and ΔH,
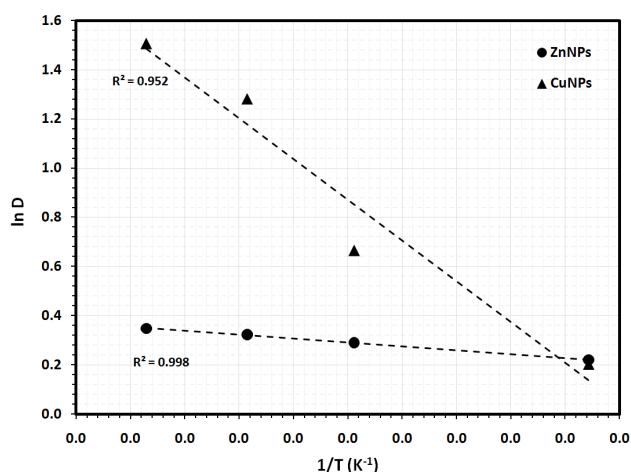

Fig. 13. Plot of $\ln D$ vs. $1/T$ for the thermodynamic parameters calculations for the AR dye removal from an aqueous solution by ZnNPs and CuNPs. .

Table 2
Removal capacity of different acid red dye by various removal processes

Material	Dye	Removal capacity (mg/g)	Time (min)	Removal technique	Reference
ZnNPs	Acid Red 1	8.84	30	Catalytic degradation	Present work
CuNPs	Acid Red 1	12.73	30	Catalytic degradation	Present work
Wheat bran modified	Acid Red 18	49.12	180	Adsorption	[37]
Surfactant modified clinoptilolite zeolite	Acid Red 18	11 mg/g	150	Adsorption	[38]
Organic-bentonite	Acid red 73	6.5	120	Adsorption	[39]
montmorillonite	Acid Red 18	50	5	Photo catalytic degradation	[40]
Iron impregnated biochars	acid red 1	10	120	Fenton	[41]
Fe(II)-Y Zeolite	Acid Red 14	3.3	6	Fenton	[42]
BiOI/ZnO nanocomposite	Acid red 18	39.1	60	Photo degradation	[43]
Cobalt doped titanianano material	Acid red 18	5	60	Photo degradation	[44]

ΔS, and ΔG values were +2.63 kJ/mole, +11.3 J/mole·K, and –0.719 kJ/mole at 298 K, respectively. Thermodynamic parameters for the AR dye molecules removed by the CuNPs were calculated, and ΔH, ΔS, and ΔG values were +27.6 kJ/mole, +99.6 J/mole·K, and –2.12 kJ/mole at 298 K, respectively. The positive value of the enthalpy change indicated the endothermic nature of the AR dye by the both ZnNPs, and CuNPs, and the positive value of the entropy change indicated the increase in the degree of freedom at the solid–liquid interface, and apparently the negative value of the free energy change as would be expected for a product favored and spontaneous removal process. Accordingly, the negative value of ΔG, and positive values of ΔH, and ΔS suggested that the removal of AR dye by the NPs from aqueous solution is an entropy-driven process. Also, according to the ΔG values, it is clear that the removal of the AR dye is more spontaneous by the CuNPs compared with the ZnNPs.

3.5. The removal mechanism

The reaction between AR dye and NPs such as ZnNPs, and CuNPs is well known and studied, as the NPs works as electron donors and the AR dye molecules work as electron acceptors. Accordingly, the NPs reduced in the aqueous medium and produced hydroxyl, hydrogen ions which react with dye molecules to induce the break of chromophore bond of –N=N– bond which degrade the AR dye molecules [14,21,26]. The degradation of AR dye molecules through reductive catalytic pathway was monitored through TOC analysis. The % TOC; total organic carbon, in the solution with time were measured during the catalytic degradation process of the AR dye by ZnNPs and CuNPs as it is shown in Fig. 14. It is observed that the decrease in the % AR dye in solution was associated with the same decrease trend of the % TOC in solution for both NPs. In the case of using ZnNPs, the % AR dye in solution decreased to around 41.6% within 10 min associated with % TOC in water of 47.5%, and this percentage was decreased to 40.0% after 60 min with a % AR dye in the solution of 33.7%. The same trend was observed in the case of using CuNPs, the % AR dye in solution decreased to around 11.0 % within 10 min associated with % TOC in water of 27.6%, and this % was decreased to 10.0% after 60 min with a % AR dye in the solution of 5.0%. This may indicate the successful removal of the AR dye by both ZnNPs and CuNPs through reductive catalytic degradation pathway, which agrees well with previous studies used different zero valent metallic nanoparticles for the reductive catalytic degradation of different dyes in water [19–28,33–36].

3.6. Environmental applications

The removal of AR dye from real wastewater sample by ZnNPs and CuNPs was performed to investigate the applicability of the proposed NPs. A wastewater sample was collected from the membrane bio-reactor technology waste water treatment plant ((MBR 6000 STP) at King Abdulaziz University (KAUWW), Jeddah City (Latitude deg. North 21.487954, Longitude deg. East 39.236748). The concentration of the AR dye was measured initially, was below the detection limit. Therefore, the samples were spiked by a concentrated AR dye solution to obtain a final concentration of 20 mg/L. Fig. 15 shows the variation of % AR dye removed from the
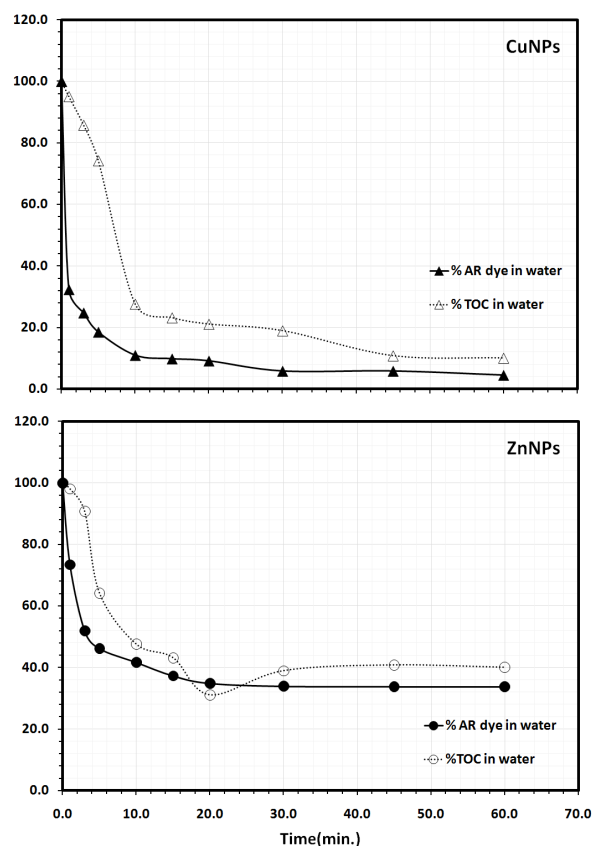

Fig. 14. Variation of the % AR dye and % TOC in water with time for the removal of AR dye by ZnNPs and CuNPs from aqueous solution. (Experimental conditions: 30.0 mg ZnNPs, 20.0 mg CuNPs, 20.0 ml solution, pH 8.0, and AR dye concentration 20.0 mg L^{-1}).
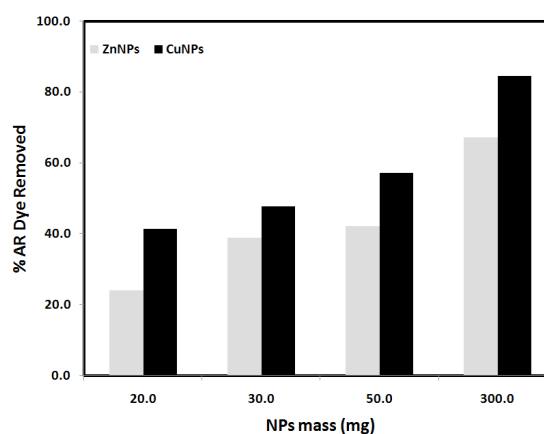

Fig. 15. The variation of % AR dye removed from the wastewater sample with the mass of both ZnNPs, and CuNPs.(Experimental conditions: 20.0 ml solution, pH 8.0, and AR dye concentration 20.0 mg L^{-1})

wastewater sample with the mass of both ZnNPs and CuNPs. It is clear that the % AR dye removed was enhanced considerably by increasing the mass of the NPs until most of the AR dye was removed using 300 mg NPs. This is much more than

what was obtained using ZnNPs or CuNPs with the model solution. This is due to the fact that wastewater usually contains different types of pollutants and not only the proposed dye, and consequently those pollutants interact with the NPs and decrease the efficiency of the AR dye removal.

4. Conclusions

The removal of the AR dye from an aqueous solution using different zero-valent metal nanoparticles; ZnNPs, and CuNPs, was studied. The ZnNPs and CuNPs were synthesized first using sodium borohydride, and characterized using different characterization techniques. The characterization results showed that ZnNPs exist in the form of Wurtzite structure of zincite, as agglomeration of spherical nanoparticles with an average diameter of 200 nm, and specific surface area of 16.1 m^2/g, whereas CuNPs exist as face-centered cubic zero-valent copper crystal, elongated double-cone in shape with an average diameter of 50 nm, and specific surface area of 71.3 m^2/g. The effect of different environmental conditions, NPs mass, removal time, and solution temperature were investigated. The experimental results revealed that AR dye removal increased gradually with increasing the amount of NPs used, removal time, and raising the solution temperature. The optimized conditions for optimal removal were 80 mg ZnNPs, and 30 mg of CuNPs, within 10.0 min at room temperature. The removal of the AR dye using ZnNPs, and CuNPs, was studied kinetically and thermodynamically, and the results showed that the experimental data were best fitted using the pseudo-second-order kinetic model with excellent correlation coefficients. The thermodynamic study of the removal process showed that the endothermic nature (positive value of ΔH), and spontaneity (negative value of ΔG) of the removal process, with an increase in the degrees of randomness (positive value of ΔS), indicating that the removal of the AR dye by ZnNPs, and CuNPs is entropy driving process. The mechanism of the removal process was studied and the results showed that the removal process occurred via reductive catalytic degradation of the AR dye molecules by both NPs, as they work as electron donor and the dye molecules works as electron acceptor, which lead to the produce of hydroxyl, hydrogen ions which react with dye molecules to induce the break of chromophore bond of –N=N– bond which degrades the AR dye molecules The applicability of the ZnNPs, and CuNPs for removal of AR dye in real wastewater sample contains AR dye, and the results showed the high removal efficiency.

Acknowledgements

References

[1] A. Lewinsky, Hazardous materials and wastewater: Treatment, Removal and Analysis, Nova Publishers – Nature, 2007, 150 p.

[2] S. Couto, Dye removal by immobilised fungi, Biotechnol. Adv., 27 (2009) 227–235.

[3] N. Mathur, P. Bhatnagar, Mutagenicity assessment of textile dyes from Sanganer (Rajasthan), J. Environ. Biol., 28 (2007) 123–126.

[4] R. Abraham, H.S. Freeman, Environmental chemistry of dyes and pigments, John Wiley & Sons, 1996.

[5] M.S. Siboni, A. Khataee, F. Vafaei, S.W. Joo, Comparative removal of two textile dyes from aqueous solution by adsorption onto marine-source waste shell: Kinetic and isotherm studies, Korean J. Chem. Eng., 31 (2014) 1451–1459.

[6] A. Mohagheghian, R.V. Kolur, M. Pourmohseni, J.K. Yang, M.S. Siboni, Application of scallop shell-Fe_3O_4 nano-composite for the removal azo dye from aqueous solution, Water, Air, Soil Pollut., 226 (2015) 321.

[7] A. Mohagheghian, S.A. Karimi, J.K. Yang, M. Shirzad-Siboni, Photo catalytic degradation of a textile dye by illuminated tungsten oxide nanopowder, J. Adv. Oxid. Technol., 18 (2015) 61–68.

[8] V. Katheresan, J. Kansedo, S.Y. Lau, Efficiency of various recent wastewater dye removal methods: A review, J. Environ. Chem. Eng., 6 (2018) 4676–4697.

[9] J. Cao, L. Wei, Q. Huang, L. Wang, S. Han, Reducing degradation of azo dyes by zero-valent iron in aqueous solution, Chemosphere, 38 (1999) 565–571.

[10] A. Khan, S.M. Prabhu, J. Park, W. Lee, C-M. Chon, J.S. Ahn, G. Lee, Azo dye decolorization by ZVI under circum-neutral pH conditions and the characterization of ZVI corrosion products, J. Ind. Eng. Chem., 47 (2017) 86–93.

[11] M.R. Sohrabi, M. Moghri, H.R.F. Masoumi, S. Amiri, N. Moosavi, Optimization of reactive blue 21 removal by nanoscale zero-valent iron using response surface methodology, Arab. J. Chem., 9 (2016) 518–525.

[12] N. Ahuja, A.K. Chopra, A.A. Ansari, Removal of colour from aqueous solutions by using zero-valent iron nanoparticles, IOSR J. Environ. Sci. Toxicol. Food Technol., 10 (2016) 04–14.

[13] M.R. Samarghandi, M. Zarrabi, A. Amrane, M.N. Sepehr, S. Namdari, Kinetic of degradation of two azo dyes from aqueous solutions by zero iron powder: determination of the optimal conditions, Desal. Water Treat., 40 (2012) 137–143.

[14] C. Raman, S. Kanmani, Textile dye degradation using nano zero-valent iron: A review, J. Environ. Manage., 15 (2016) 341–355.

[15] H-Y. Shu, M-C. Chang, J-J. Liu, Reductive decolorization of acid blue 113 azo dye by nanoscale zero-valent iron and iron-based bimetallic particles, Desal. Water Treat., 57 (2016) 7963–7975.

[16] X. Sun, T. Kurokawa, M. Suzuki, M. Takagi, Y. Kawase, Removal of cationic dye methylene blue by zero-valent iron: Effects of pH and dissolved oxygen on removal mechanisms, J. Environ. Sci. Health., Part A., 50 (2015) 1057–1071.

[17] S. Dutta, R. Saha, H. Kalitab, A.N. Bezbaruah, Rapid reductive degradation of azo and anthraquinone dyes by nanoscale zero-valent iron, Environ. Technol. Innov., 5 (2016) 176–187.

[18] P. Liu, J. Keller, W. Gernjak, Enhancing zero-valent iron based natural organic matter removal by mixing with dispersed carbon cathodes, Sci. Total Environ., 550 (2016) 95–102.

[19] Y.H. Kim, E.R. Carraway, Dechlorination of chlorinated phenols by zero-valent zinc, Environ. Technol., 24 (2003) 1455–1463.

[20] A.J. Salter-Blanc, E.J. Suchomel, J.H. Fortuna, J.T. Nurmi, Ch. Walker, T. Krug, S. O'Hara, N. Ruiz, Th. Morley, G. Paul, Evaluation of zero-valent zinc for treatment of 1,2,3-trichloropropane-contaminated groundwater: laboratory and field assessment, Tratnyek Ground, Water Monit. Rem., 32 (2012) 42–52.

[21] Y. Han, Z. Chen, L. Tong, L. Yang, J. Shen, B. Wang, Y. Liu, Y. Liu, Q. Chen, Reduction of N-nitrosodimethylamine with zero-valent zinc, Water Res., 47 (2013) 216–224.

[22] V.K. Vidhu, D. Philip, Catalytic degradation of organic dyes using biosynthesized silver nanoparticles, Micron., 56 (2014) 54–62.

[23] N.R. Jana, T.K. Sau, T. Pal, Growing small silver particle as redox catalyst, J. Phys. Chem. B., 103 (1999) 115–121.

[24] M.A. Mekewi, A.S. Darwish, M.S. Aminutes, Gh. Eshaq, H.A. Bourazan, Copper nanoparticles supported onto montmoril-lonite clays as efficient catalyst for methylene blue dye degra-dation, Egypt. J. Pet., 25 (2016) 269–279.

[25] T. Sinha, M. Ahmaruzzaman, Green synthesis of copper nanoparticles for the efficient removal (degradation) of dye from aqueous phase, Environ. Sci. Pollut. Res., 22 (2015) 20092–20100.

[26] P. Li, Y. Song, Sh. Wangb, Z. Tao, Sh. Yu, Y. Liu, Enhanced decolorization of methyl orange using zero-valent copper nanoparticles under assistance of hydrodynamic cavitation, Ultrason. Sonochem., 22 (2015) 132–138.

[27] R.A. Soomro, A. Nafady, Sirajuddin, S.T.H. Sherazi, N.H. Kalwar, M.R. Shah, K.R. Hallam, Catalytic reductive degra-dation of methyl orange using air resilient copper nanostruc-tures, J. Nanomater., Article ID 136164 (2015) 12. http://dx.doi.org/10.1155/2015/136164.

[28] T. Kamal, Sh. B. Khan, A.M. Asiri, Synthesis of zero-valent Cu nanoparticles in the chitosan coating layer on cellulose micro-fibers: evaluation of azo dyes catalytic reduction, Cellulose, 23 (2016) 1911–1923.

[29] European Food Safety Authority, Opinion of the scientific panel on food additives, flavourings, processing aids and materials in contact with food (AFC) on hydrocyanic acid in flavourings and other food ingredients with flavouring prop-erties, EFSA J., 515 (2007) 1–28.

[30] Y.S. Ho, Review of second-order models for adsorption sys-tems, J. Hazard. Mater., 136 (2006) 681–689.

[31] V. Bagdonavicius, M.S. Nikulin, Chi-square goodness-of-fit test for right censored data, Int. J. Appl. Math. Stat., 24 (2011) 30–50.

[32] M.A. Salam, Coating carbon nanotubes with crystalline man-ganese dioxide nanoparticles and their application for lead ions removal from model and real water, Colloids Surf. A., 419 (2013) 69–79.

[33] S. Yihan, L. Mingming, Z. Guo, Ag nanoparticles loading of polypyrrole-coated super wetting mesh for on-demand sep-aration of oil-water mixtures and catalytic reduction of aro-matic dyes, J. Colloid Interface Sci., 527 (2018) 187–194.

[34] M. Ismail, M.I. Khan, S.B. Khan, K. Akhtar, M.A. Khan, A. M. Asiri, Catalytic reduction of picric acid, nitrophenols and organic azo dyes via green synthesized plant supported Ag nanoparticles, J. Mol. Liq., 268 (2018) 87–101.

[35] S.A. A.Vandarkuzhali, S. Karthikeyan, B. Viswanathan, M.P. Pachamuthu,Arachishypogaea derived activated carbon/Pt catalyst: Reduction of organic dyes, Surf. Interfaces, 13 (2018) 101–111.

[36] Md. T. Islam, N. Dominguez, Md. A. Ahsan, H. D-Cisneros, P. Zuniga, P.J.J. Alvarez, J.C. Noveron, Sodium rhodizonate induced formation of gold nanoparticles supported on cellu-lose fibers for catalytic reduction of 4-nitrophenol and organic dyes, J. Environ. Chem. Eng., 5 (2017) 4185–4193.

[37] W-X. Zhang, L. Lai, P. Mei, Y. Li, Y-H. Li, Y. Liu, Enhanced removal efficiency of acid red 18 from aqueous solution using wheat bran modified by multiple quaternary ammonium salts, Chem. Phys. Lett., 710 (2018) 193–201.

[38] N. Mirzaei, H.R. Ghaffari, K. Sharafi, A. Velayati, G. Hosein-doost, S. Rezaeie, A. Hossein, M.A. Azarif, K. Dindarloo,-Modified natural zeolite using ammonium quaternary based material for Acid red 18 removal from aqueous solution, J. Environ. Chem. Eng., 5 (2017) 3151–3160.

[39] X. Wang, X. Gong, B. Yu, Adsorption behavior of organically modified bentonite for acid brilliant scarlet GR, Adv. Mater. Res., 554–556 (2012) 2089–2092.

[40] C. Zhang, Y. Yu, H. Wei, K. Li, In situ growth of cube-like AgCl on montmorillonite as an efficient photo catalyst for dye (Acid Red 18) degradation, Appl. Surf. Sci., 456 (2018) 577–585.

[41] K.K. Rubeena, P.H.P. Reddy, A.R. Laiju, P.V. Nidheesh, Iron impregnated biochars as heterogeneous Fenton catalyst for the degradation of acid red 1 dye, J. Environ. Manage., 226 (2018) 320–328.

[42] R. Idel-aoud, M. Valiente, A. Yaacoubi, B. Tanouti, M. López-Mesas, Rapid decolourization and mineralization of the azo dye C.I. Acid Red 14 by heterogeneous Fenton reaction J. Hazard. Mater., 186 (2011) 745–750.

[43] S. Jorfi, M.J. Barkhordari, M. Ahmadi, N. Jaafarzadeh, A. Moustofi, B. Ramavandi, Photo degradation of Acid red 18 dye by BiOI/ZnO nanocomposite: A dataset, Data in Brief, 16 (2018) 608–611.

[44] R.D. Chekuri, S.R. Tirukkovalluri, Synthesis of cobalt doped titanianano material assisted by gemini surfactant: Charac-terization and application in degradation of Acid Red under visible light irradiation, South Afr. J. Chem. Eng., 24 (2017) 183–195.